Density Functional Theory Study of Formic Acid Adsorption on Anatase TiO_2(001): Geometries, Energetics, and Effects of Coverage, Hydration, and Reconstruction

Xue-Qing Gong,*,† Annabella Selloni,† and Andrea Vittadini‡

Department of Chemistry, Princeton University, Princeton, New Jersey 08544, Dipartimento di Scienze Chimiche, Università di Padova, Padova, Italy, and Istituto di Scienze e Tecnologie Molecolari, Consiglio Nazionale delle Ricerche di Padova, Padova, Italy

Received: November 14, 2005; In Final Form: December 2, 2005

We present density functional theory calculations and first-principles molecular dynamics simulations of formic acid adsorption on anatase TiO_2(001), the minority surface exposed by anatase TiO_2 nanoparticles. A wide range of factors that may affect formic acid adsorption, such as coverage, surface hydration, and reconstruction, are considered. It is found that (i) formic acid dissociates spontaneously on unreconstructed clean TiO_2(001)-1 × 1, as well as on the highly reactive ridge of the reconstructed TiO_2(001)-1 × 4 surface; (ii) on both the 1 × 1 and 1 × 4 surfaces, various configurations of dissociated formic acid exist with adsorption energies of about 1.5 eV, which very weakly depend on the coverage; (iii) bidentate adsorption configurations, in which the formate moiety binds to the surface through two Ti−O bonds, are energetically more favored than monodentate ones; (iv) partial hydration of TiO_2(001)-1 × 1 tends to favor the bidentate chelating configuration with respect to the bridging one but has otherwise little effect on the adsorption energetics; and (v) physical adsorption of formic acid on fully hydrated TiO_2(001)-1 × 1 is also fairly strong. Comparison of the present results for formic acid adsorption with those for water and methanol under similar conditions provides valuable insights to the understanding of recent experimental results concerning the coadsorption of these molecules.

1. Introduction

Titanium dioxide (TiO_2) is a material of paramount importance in a wide range of applications, such as photocatalysis, solar cells, gas sensors, biomaterials, and memory devices.[1−7] Among its most common polymorphs, that is, rutile, anatase, and brookite, anatase TiO_2 has attracted great interest since it exhibits higher activity in many cases.[1,2] Moreover, experimental and theoretical studies have shown that TiO_2 nanoparticles with size up to ∼14 Å prefer the metastable anatase phase rather than the rutile form, which is the most stable for bulk TiO_2.[8−11] To gain insight into the reactivity of anatase TiO_2 nanoparticles, interactions of prototype molecules, such as water, methanol, and other simple organic molecules, with anatase surfaces have been widely studied.[11−43] In this regard, work on formic acid, the simplest organic acid, is of particular interest.[20,23−25,39] Besides its obvious importance in biochemistry, as one of the building blocks of amino acids, the carboxylic group is also the key functional group used to bind photosensitizers to TiO_2.[24,39,44−47]

The anatase TiO_2 nanoparticles used in many photocatalytic applications and particularly in solar cell devices most frequently expose (101) or (100) majority surfaces, together with small (001) facets.[8,11,48−53] Work on these different crystal facets suggests that the minority (001) surface is more reactive than the majority surfaces and plays a key role in the reactivity of anatase nanoparticles.[8,11,35,38,40,43,48−53] Investigation of formic acid adsorption on anatase TiO_2(001) may be thus important for a better understanding of dye-sensitized nanostructured materials.[2,45−47]

Extensive investigations on rutile TiO_2(110) have demonstrated dissociative adsorption, with formate (HCOO) adsorbing in two types of bidentate bridging configurations.[24,54−60] By contrast, work on anatase TiO_2 surfaces is more limited, and conclusive results regarding the geometries and energetics of formic acid on anatase have not been reached yet.[22,24,25,39,61,62] Some early experimental studies employing temperature-programmed desorption (TPD) measurements on anatase TiO_2 powders showed that formic acid can adsorb both molecularly and dissociatively.[61,62] Popova et al.,[25] by using in situ fast Fourier transform infrared (FTIR) spectroscopy, studied the adsorption of formic acid on anatase TiO_2 samples with surface area of about 100 m^2/g. Evidence of dissociative adsorption and information regarding various formate adsorption geometries was reported. Using density functional theory (DFT) calculations, Vittadini et al.[39] studied formic acid adsorption on both clean and hydrated anatase TiO_2(101). Their results indicate that the adsorption is purely molecular on the clean surface, while dissociation is favored on the hydrated one, the adsorption being rather weak in both cases. This seems inconsistent with experiments showing that dissociated formic acid is stable on anatase particles at temperatures even higher than 200 °C,[25] which again suggests that the (101) surface may not be responsible for the observed activity of anatase nanoparticles.[43] Using atomic resolution scanning tunneling microscopy (STM) and noncontact atomic force microscopy (NC-AFM), Tanner et al.[24] studied formic acid adsorption on the (1 × 4) reconstructed TiO_2(001) surface. They proposed that formic acid dissociatively adsorbs at the "ridges" (a special structural motif of the reconstructed surface, see below), giving rise to an

* To whom correspondence should be addressed: fax +1-(609)-258-6746; e-mail xgong@princeton.edu.
† Princeton University.
‡ Università di Padova and CNR di Padova.

10.1021/jp056572t CCC: $33.50
Published on Web 01/21/2006

adsorption structure in which the molecular plane of surface formate is parallel to the ridge row.[24] More recently, Shultz and co-workers[22] systematically compared the adsorption of acetic acid, water, and methanol on anatase TiO_2 colloidal nanoparticles by using sum frequency generation (SFG) vibrational spectroscopy. They found that water and methanol have a similar adsorption behavior, and depending on their partial pressure, they can actually displace each other from the surface. By contrast, acetic acid (CH_3COOH), whose properties are expected to be very similar to those of formic acid (HCOOH), can easily and *irreversibly* replace dissociated water and methanol.

To obtain detailed structural and energetic information about formic acid adsorption on anatase TiO_2, which could help in understanding the available experimental results, we have carried out systematic density functional theory (DFT) calculations and first-principles molecular dynamics (MD) simulations[63] of formic acid adsorption on anatase TiO_2(001). Key factors that may affect adsorption, namely, the coverage and the surface hydration and reconstruction, are considered. The results are further compared with previous calculations as well as with experimental findings concerning water and methanol adsorption on anatase surfaces. It is found that the dissociative adsorption of formic acid is highly favored on anatase TiO_2(001) under different conditions, and bidentate configurations are always energetically preferred to monodentate ones. Moreover, formic acid adsorption is much stronger than that of water and methanol regardless of coverage, surface hydration, and reconstruction.

2. Calculations

2.1. Methods. Calculations have been performed with slab geometries and a periodic DFT approach within the generalized gradient approximation.[64a] Structural optimizations and MD simulations have been performed within the Car-Parrinello (CP) approach.[63] Electron−ion interactions are described by ultrasoft pseudopotentials,[64b] with electrons from C and O 2s, 2p and Ti 3s, 3p, 3d, and 4s shells explicitly included in the calculations. Plane-wave basis set cutoffs for the smooth part of the wave functions and the augmented density are 25 and 200 Ry, respectively. *k*-Point sampling is restricted to the Γ point.

The anatase TiO_2(001) surface was modeled as a periodic slab with four layers of oxide (∼8 Å thick), while the vacuum between slabs was ∼10 Å wide. For the 1 × 1 surface, a p(3 × 2) surface supercell was used, with a surface area of 11.36 × 7.57 Å^2. For the reconstructed anatase TiO_2(001)-1 × 4 surface, we adopted the model proposed in ref 65 and used a p(2 × 4) surface cell. Only one side of the slab was reconstructed or hydrated and subsequently used for adsorption simulations. In all calculations, the atoms in the bottom layer were fixed to their bulk truncated position, while all the other atoms were allowed to relax/move. Geometry optimizations were carried out through damped molecular dynamics until the largest component in the forces on all mobile atoms was below 0.05 eV/Å. In the MD simulations, a time step of 0.145 fs and a fictitious electronic mass of 700 atomic units (amu) and a 2 amu hydrogen mass were used. The ionic temperatures were controlled by means of a Nosè thermostat.[66]

2.2. Surface Energies. The surface energy (γ) of the clean surface was computed by use of the PWSCF code,[67] which is part of the same (ESPRESSO) package that includes also the CP code. For clean anatase TiO_2(001)-1 × 1 and 1 × 4 surfaces, we used the expression $\gamma = (E_{slab} - nE_{TiO_2})/A$, where E_{slab} is the total energy of the slab, E_{TiO_2} is the energy of a TiO_2 unit in the bulk, n is the number of TiO_2 units in the slab, and A is the total exposed area, including both sides of the slab. To determine the energy of bulk anatase, we considered the primitive cell containing four TiO_2 units and used a 4 × 4 × 2 mesh of *k*-points to sample the Brillouin zone. The TiO_2(001)-1 × 1 surface was modeled by a slab of four layers of oxide and a p(1 × 1) unit cell was used (4 TiO_2 units in a cell). The TiO_2(001)-1 × 4 surface was modeled by four layers of oxide and a p(1 × 4) super cell was used with the ADM model[65] on both surfaces of the slab (18 TiO_2 units in a cell). Meshes of 4 × 4 × 1 and 4 × 1 × 1 *k*-points were used for the (001)-1 × 1 and (001)-1 × 4 surfaces, respectively. All the atoms were allowed to relax (force threshold = 0.03 eV/Å). In this way we obtain $\gamma = 0.98$ J·m^{-2} for the clean anatase TiO_2(001)-1 × 1 surface and $\gamma = 0.48$ J·m^{-2} for the reconstructed 1 × 4 surface. The estimated errors on these values, about ±0.05 J·m^{-2}, are due to both the dependence of γ on the value of the bulk energy E_{TiO_2} and the rather small thickness of our slabs.

To evaluate the surface energy of the hydrated surface (γ'), we used the expression $\gamma' = \gamma - nE_d/A'$, where γ is the surface energy of clean surface, E_d is the adsorption energy of dissociated water,[43] n is the number of adsorbed water molecules in a unit cell (n = 2 and 3 at $^1/_3$ and $^1/_2$ ML coverage on 1 × 1 surface, respectively), and A' is the area of one surface of the slab (11.36 × 7.57 Å^2; $A' = {}^1/_2A$). Using the values of E_d reported in ref 43, which are referred to a water molecule in the *gas phase*, we obtain $\gamma' = 0.33$ and 0.57 J·m^{-2} for the fully ($^1/_2$ ML) and partially ($^1/_3$ ML) hydrated anatase TiO_2(001)-1 × 1 surfaces, respectively. We also calculated the water adsorption energy by taking a water molecule in *liquid water* as the reference. For the surface energy of the hydrated surface (γ''), we then used the expression $\gamma'' = \gamma - (nE_d - n\Delta H)/A'$, where ΔH is the enthalpy of vaporization of water. From tabulated values, we estimate $\Delta H \sim 0.45$ eV (43.5 kJ·mol^{-1}) at room temperature.[68] Accordingly, we obtain $\gamma'' = 0.58$ and 0.73 J·m^{-2} for the fully and partially hydrated anatase TiO_2(001)-1 × 1 surfaces, respectively. It is still evident that hydration significantly stabilizes the clean TiO_2(001)-1 × 1 surface ($\gamma = 0.98$ J·m^{-2}). Moreover, the 1 × 4 reconstructed surface ($\gamma = 0.48$ J·m^{-2}) has very similar stability compared to the fully hydrated TiO_2(001)-1 × 1.

3. Clean and Hydrated (001) Surfaces

3.1. Clean Anatase TiO_2(001): 3.1.1. 1 × 1 Structure. On the clean anatase TiO_2(001)-1 × 1 surface, fully coordinated 3-fold oxygens (O_{3c}), together with coordinatively unsaturated (cus)[69,70] 5-fold Ti (Ti_{5c}) and 2-fold O (O_{2c}) are present (see Figure 1a). For this surface, the calculated surface energy of 0.98 J·m^{-2} (see section 2.2) is nearly twice that of the most stable anatase (101) surface (∼0.5 J·m^{-2}).[52] Accordingly, first-principles calculations show that the anatase (001) surface is considerably more reactive than the (101) one. For instance, water and methanol are found to dissociatively adsorb on anatase TiO_2(001)-1 × 1,[14,40,43] whereas molecular adsorption takes place on the majority (101) surface, even though Ti_{5c} and O_{2c} also exist on the latter.[35,36,40]

These differences between the (101) and (001) surfaces can be understood in terms of their electronic structures.[43] The O_{2c} atoms on (001) have higher energies compared to the bulk O_{3c}, while O_{2c} and bulk O_{3c} of anatase (101) appear to have very similar stabilities. This suggests that the high reactivity of anatase (001) is associated with O_{2c} atoms.

3.1.2. 1 × 4 Structure. It was found a few years ago that carefully annealed anatase TiO_2(001) surfaces under UHV conditions exhibit a 1 × 4 reconstruction.[71−73] In Figure 1b,

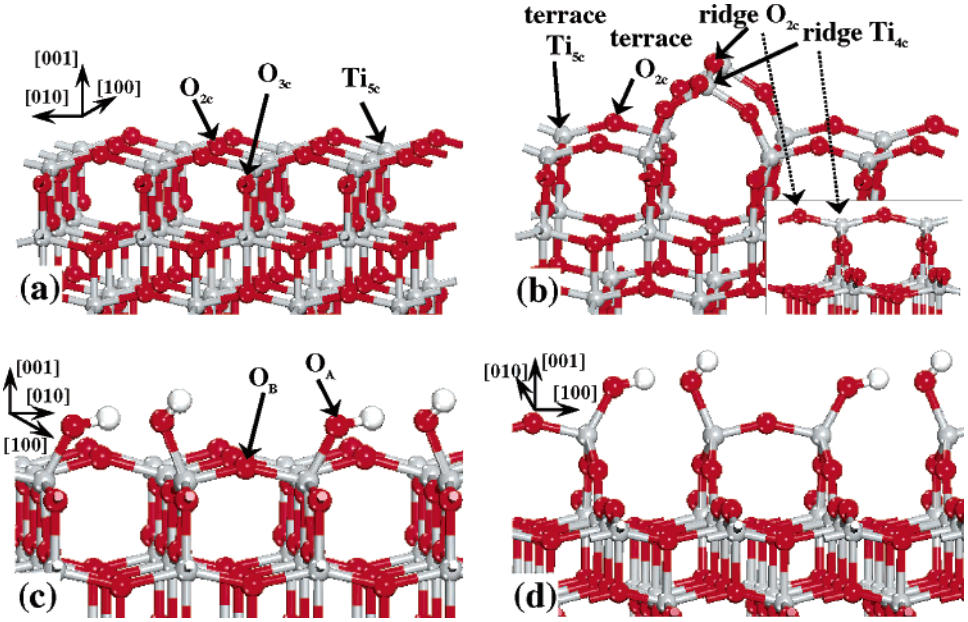

Figure 1. (Top) Structures of (a) clean anatase TiO_2(001)-1 × 1 and (b) clean anatase TiO_2(001)-1 × 4. (Bottom) Structures of (c) hydrated anatase TiO_2(001)-1 × 1 at water coverage of $^1/_6$ ML and (d) hydrated anatase TiO_2(001)-1 × 4. O atoms are red, Ti atoms are light gray, and H atoms are white. This notation is used throughout this paper.

we show the reconstructed surface on the basis of the so-called ADM model,[65] which is currently accepted as the one that best describes the available experimental information. By comparing structures a and b in Figure 1, one may notice that this 1 × 4 structure is constructed by periodically replacing rows of surface bridging oxygen atoms (O_{2c}) of the unreconstructed 1 × 1 structure with rows of TiO_3 species.[65] Then, on this bridging TiO_3 chain (ridge), each Ti atom (Ti_{4c}) binds to four oxygen atoms only and is therefore highly coordinatively unsaturated. Despite this, the computed surface energy of the reconstructed (001)-1 × 4 surface in Figure 1b is 0.48 J·m^{-2}, nearly half that of (001)-1 × 1 (see section 2.2), indicating that this reconstruction can indeed stabilize the surface quite effectively. As proposed in ref 65, the stability of the ADM surface structure can be explained by the fact that it leads to a strong relief of the surface stress. Indeed, the $Ti_{5c}-O_{2c}$ bonds on the terrace of the reconstructed surface have lengths of 1.80−1.85 Å, while those on the original 1 × 1 surface are ∼1.96 Å, indicating increased strength of those terrace bonds (see Supporting Information for a complete list of structural parameters and charge-density distribution contour plots of the surfaces before and after reconstruction).

As a consequence of the stronger surface bonds, the cus Ti_{5c} and O_{2c} atoms on the terrace of the reconstructed surface should also become much less reactive. This is confirmed by the electronic densities of states (DOS) reported in Figure 2, panels a and b, for the unreconstructed and reconstructed TiO_2(001) surfaces, respectively. In fact, the projected DOS (PDOS) curves show that the O_{2c} states, which in the case of the unreconstructed surface accumulate at the higher energy end of the valence band, are definitely stabilized for the terrace atoms of the 1 × 4 surface. From Figure 2b, one may also notice that for the reconstructed surface the edge of the valence band is mainly constituted by the states from the O_{2c} atoms at the ridges. Considering the presence of such active O_{2c} and of the highly coordinatively unsaturated Ti_{4c} as well, we expect the ridges of the reconstructed anatase 1 × 4 surface to be highly reactive.

3.2. Hydrated Anatase TiO_2(001): 3.2.1. Hydrated 1 × 1 Surface. Reconstruction is not the only mechanism of surface stabilization; on oxide surfaces, water adsorption can be very

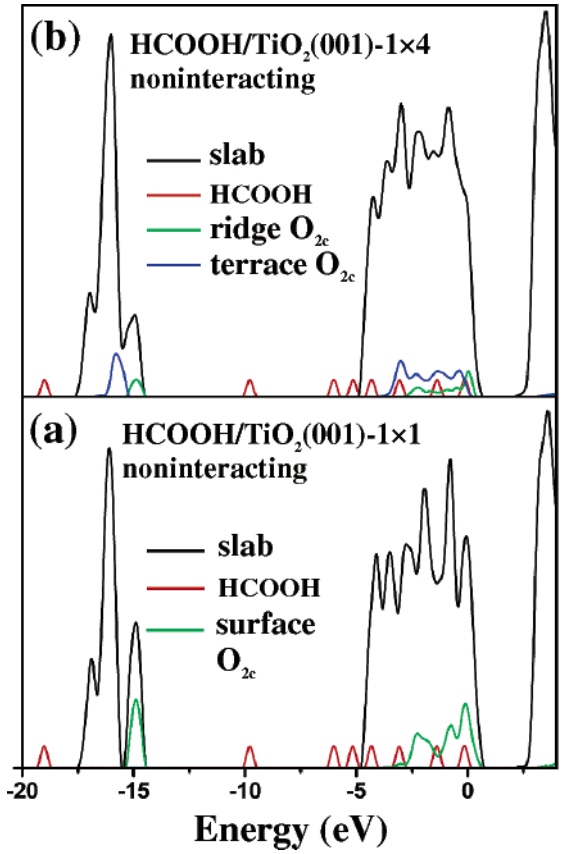

Figure 2. DOS of noninteracting (a) HCOOH/TiO_2(001)-1 × 1 and (b) HCOOH/TiO_2(001)-1 × 4 systems. The curves in top and bottom plots are aligned by matching the HOMO of gas-phase HCOOH.

effective as well.[12,14,43,74] On the TiO_2(001)-1 × 1 surface, in fact, dissociatively adsorbed water significantly decreases the surface energy, from 0.98 J·m^{-2} for the clean surface to 0.57 and 0.33 J·m^{-2} at water coverages $\theta_{H_2O} = {}^1/_3$ and $^1/_2$ ML, respectively (see section 2.2).[43] The mechanism of surface stabilization through dissociative adsorption of water, or similar molecules such as methanol, can be understood as follows.[43]

TABLE 1: Structural Parameters and Adsorption Energies of Dissociated Formic Acid on Clean Anatase TiO_2(001)-1 × 1 at $^1/_6$ ML Coverage[a]

	$Ti_{5c}-O_f$ (Å)	$Ti_{5c}-O_{2c}$ (Å)	Ti_{5c}*$-O_{2c}$ (Å)	$O_{2c}-H_f$ (Å)	O_f*$-H_f$ (Å)	E_a (eV)	Figure
M-Hup	2.049	2.351	1.861	1.098	1.344	1.19	3a
M-Oup	1.935	3.539	1.756	1.025	1.512	1.09	3b
BC	2.233	2.379	1.898	0.997		1.45	3c
BB1	2.039	2.393	1.929	0.987		1.54	3d
BB2	2.018		1.857	0.988		1.68	3f

[a] Ti_{5c} is the surface Ti atom binding the formate. Ti_{5c}* is the surface Ti atom binding O_{2c}, which accepts the acidic H (H_f) from formic acid. O_f is the O of the formate that binds to Ti_{5c}. In the bidentate cases, O_f represents both O atoms of formate and $Ti_{5c}-O_f$ is the average bond distance. O_f* is the formate O of formic acid in monodentate configurations that forms an H-bond with H_f on O_{2c}. In the case of BB2, $O_{2c}-H_f$ and Ti_{5c}*$-O_{2c}$ are the bond lengths of the surface OH group and that between this OH group and the surface Ti binding it, respectively.

After water dissociation (see Figure 1c), the bridge O_{2c} (O_A) atom that accepts the H from the adsorbing H_2O breaks its bond with the nearby Ti_{5c}, which binds the OH of the same dissociated H_2O. In this way a surface hydroxyl group (O_AH) is formed. Therefore, this O_{2c} (O_A) is directly involved in H_2O dissociation and stabilized thereafter. For the other bridge O_{2c} (O_B in Figure 1c), it is not directly involved in the dissociation. However, both its Ti_{5c} neighbors are released from the stiff $O_{2c}-Ti_{5c}-O_{2c}-Ti_{5c}$ framework in the way described above and can thus form tighter bonds with O_B, as on the 1 × 4 reconstructed surface.[65] In this way, O_B is indirectly stabilized.

3.2.2. Water Adsorption on the Reconstructed 1 × 4 Surface. MD simulations show that water dissociates spontaneously upon approaching the ridge of TiO_3 units on the reconstructed 1 × 4 surface. In the most favorable adsorption structure (see Figure 1d), the OH moiety of dissociated H_2O binds to Ti_{4c} while H moves to the nearby bridging O_{2c}, so that the $O_{2c}-Ti_{4c}$ bond is broken. The resulting structure is similar to that on the 1 × 1 surface, but the corresponding adsorption energy, 1.82 eV, is nearly 0.6 eV higher,[43] indicating that the ridges are indeed highly reactive. On the terrace of the 1 × 4 surface, on the other hand, no dissociation occurs: water adsorbs molecularly with an adsorption energy of ~1.1 eV at low coverage, in line with the stabilization caused by the shorter $O_{2c}-Ti_{5c}$ surface bonds.

4. Formic Acid Adsorption on Clean (001) Surface

4.1. Formic Acid on 1 × 1 Surface: 4.1.1. Low Coverage. At $^1/_6$ ML coverage [corresponding to one HCOOH in each p(3 × 2) surface cell used for the calculations], dissociative adsorption is highly favored, and it yields several adsorption complexes. The most stable ones are shown in Figure 3, and the key structural parameters, together with the corresponding adsorption energies (E_a), are listed in Table 1.

In the monodentate ester-type configuration (denoted M-Hup in the following), dissociated formic acid is attached to the surface through the bond between the oxygen of its carbonyl group and a surface Ti_{5c} atom (see Figure 3a). Meanwhile, the O−H bond of its hydroxyl group is broken and H adsorbs on a surface O_{2c}, even though a strong H-bond, 1.344 Å, remains between this H and the adsorbed formate. After accepting the H, the bridge O_{2c} moves slightly away from the surface plane and the distance between it and the nearby Ti_{5c} binding the formate is increased from ~1.96 to 2.351 Å. The adsorption energy for this structure is E_a = 1.19 eV.

Another monodentate structure, more similar to that of dissociatively adsorbed water in Figure 1c, is shown in Figure 3b and will be denoted M-Oup in the following. The adsorption energy for this configuration, 1.09 eV, is somewhat smaller compared to that of M-Hup.

The bidentate chelating configuration (BC), shown in Figure 3c, has no H-bond between the formate and the $O_{2c}H$ group.

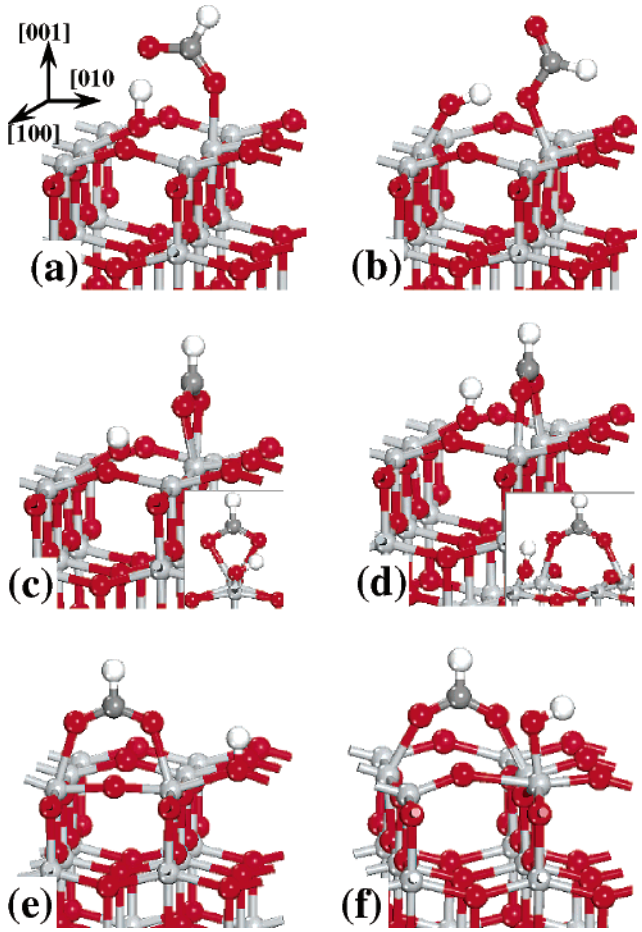

Figure 3. Structures of dissociated formic acid on clean anatase TiO_2(001)-1 × 1 at low ($^1/_6$ ML) coverage: (a) monodentate ester-type (M-Hup), (b) monodentate O-up (M-Oup); (c) bidentate chelating (BC); (d) bidentate bridging (BB1); (e) bidentate bridging above O_{2c}; (f) bidentate bridging (BB2). The C atoms are gray (this notation is used throughout this paper).

Both oxygens of the formate bind to the same Ti_{5c} and the $Ti_{5c}-O$(formate) bonds have an average length of 2.233 Å, while the distance between this Ti_{5c} and the O_{2c} accepting the dissociated H is 2.379 Å. The BC adsorption energy is 1.45 eV, higher than those of the monodentate forms.

The adsorption energy is even higher, 1.54 eV, for the bidentate bridging configuration in Figure 3d (denoted BB1 in the following). In this configuration, the two oxygens of the adsorbed formate bind to different Ti_{5c} atoms, and the average $Ti_{5c}-O$(formate) distance is ~2.04 Å (Table 1), which is similar to that in M-Hup, but significantly shorter than the one in BC. This Ti−O distance of ~2.04 Å is also very close to the corresponding one of dissociated formic acid in the bidentate

bridging configuration on rutile TiO_2(110), which is estimated to be ~2.08 Å.[55]

While in BB1 the two neighboring Ti_{5c} binding the formate are along the [100] direction and connected by an O_{3c}, there are other possible bridging configurations in which the formate sits on two Ti_{5c} in the [010] direction. One such bridging structure (Figure 3e) is found to be much less favored (E_a = 0.94 eV), whereas the slightly modified configuration in Figure 3f, denoted BB2 in the following, is very stable (E_a = 1.68 eV). The BB2 species clearly resembles the ADM model in Figure 1b, and similarly to the latter, its formation implies a considerable structural rearrangement: the O_{2c} that links the two Ti_{5c} binding the formate in Figure 3e moves to a Ti_{5c} on the neighboring row and accepts the acidic proton. The formation of BB2 was never observed during our MD simulations (up to 300 K).

4.1.2. High Coverage. At coverage of $^1/_3$ ML, corresponding to two HCOOH molecules in each p(3 × 2) surface cell of our calculations, we examined configurations with the two molecules in different combinations of the BC, BB1, and M-Hup structures in Figure 3. The most favorable conformation has two BB1 species with an average adsorption energy of 1.63 eV/molecule, while another with two BC molecules has an adsorption energy of 1.32 eV/molecule. Analysis of the structural parameters shows that adsorbed formates in the same configuration have very similar geometries at $^1/_6$ and $^1/_3$ ML coverages.

At the highest possible coverage of $^1/_2$ ML,[40,43] the dissociative adsorption of three HCOOH molecules in each p(3 × 2) surface cell of our calculations still appears very favorable: adsorption structures with two BB1 plus one M-Hup or BC molecules have an average adsorption energy of about 1.45 eV/molecule. In general, the coadsorbing formic acid molecules at higher coverages take configurations similar to those observed at low coverage, and BB1 is still energetically more favored, followed by BC and M-Hup.

4.1.3. Water, Methanol, and Formic Acid. Anatase TiO_2(001)-1 × 1 is very reactive toward water and methanol adsorption.[35,40,43] Particularly, unlike the anatase (101) surface, on which molecular adsorption is more favorable,[35,40] the (001) surface strongly favors dissociation. Only one type of configuration is determined for dissociated water and methanol on the (001) surface under various coverages (Figure 1c), and the adsorption energies of both molecules are similar and almost independent from coverage.[43]

Results are somewhat different for HCOOH adsorption. As previously discussed, several strongly bound configurations exist for dissociated formic acid (see Table 1). Moreover, while our MD simulations show that, similarly to water and methanol, HCOOH also dissociates spontaneously on clean TiO_2(001)-1 × 1, multiple routes exist for this process, which are different from the one of water and methanol (see below). This is probably due to the fact that the O−H bond in the carboxyl group is much weaker than that in a typical hydroxyl group of water and methanol. In addition, formic acid has also higher adsorption order with respect to water and methanol; that is, it has two O that may bind to the surface, versus the single oxygen of water and methanol.

By conducting MD calculations at temperatures as low as 160 K and from similar starting points (with the HCOOH molecule in the gas phase high above the surface), we always found that formic acid dissociates instantly upon approaching TiO_2(001)-1 × 1. During this process, the carbonyl O atom binds to Ti_{5c}, while the hydroxyl H is transferred to O_{2c}. As a result, either M-Hup or BB1 can form directly. Analogous MD calculations for water and methanol show that molecular adsorption initially takes place, and a considerable time (1.5−2.0 ps) is needed to achieve dissociation.[43] Furthermore, for water and methanol dissociation it is the same O atom involved in O−H breaking that binds to Ti_{5c}.

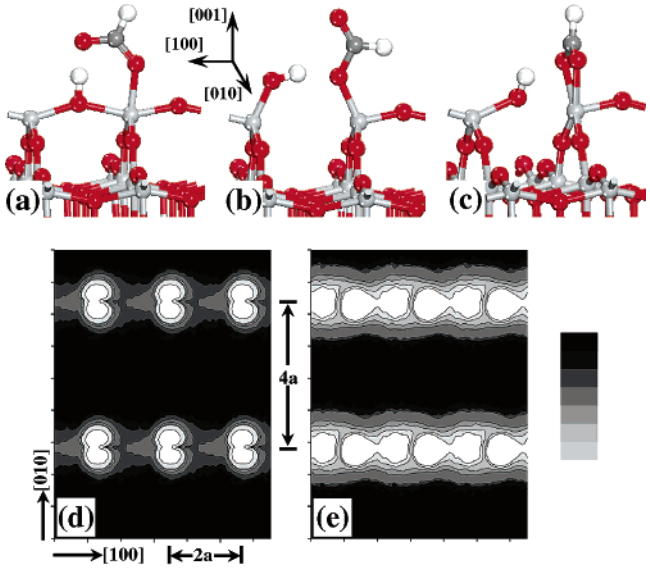

Figure 4. (Top) Structures of dissociated formic acid on the ridge of anatase TiO_2(001)-1 × 4 in (a) M-Hup, (b) M-Oup, and (c) BC configurations. (Bottom) Simulated STM images for (d) M-Oup and (e) BC species. *a* is the edge of the p(1 × 1) unit cell of anatase TiO_2(001). The images are calculated under positive sample bias conditions with a 2 eV energy window and a fixed distance of ~1 Å above the highest atom. The lighter shading corresponds to regions with denser unoccupied states.

Once formed in the MD simulation, both monodentate and bidentate HCOOH configurations remain stable even after the temperature is increased to ~300 K. This suggests that, although BB1 is more stable than M-Hup, an energy barrier needs to be overcome for M-Hup to transform to BB1. The BC species was also found to be stable during MD simulations (160 K), but this structure was never directly obtained through simulations starting with formic acid in gas phase.

4.2. Formic Acid on 1 × 4 Reconstructed Surface. Several dissociative adsorption structures analogous to those occurring on the 1 × 1 surface are found on the ridges of the reconstructed 1 × 4 surface. Figure 4a shows the structure with dissociated formic acid in monodentate ester-type, M-Hup, configuration. In this configuration, formate binds to the Ti_{4c} through a single Ti_{4c}−O(formate) bond and the H is adsorbed on a nearby O_{2c}. Structural parameters are listed in Table 2, from which one can see that the distance between the Ti_{4c} atom bonded to the formate and the O_{2c} bonded to H is only 2.086 Å, indicating the presence of a relatively strong bond. The adsorption energy is 1.31 eV, which is about 0.1 eV higher than that of formic acid in the same configuration on clean (001)-1 × 1 surface.

A larger adsorption energy, 1.66 eV, is found for the monodentate configuration M-Oup in Figure 4b, suggesting that this configuration is quite likely to occur on the 1 × 4 surface. In fact, MD simulations show that, upon starting from a HCOOH molecule high above the ridge (height > 4 Å), M-Hup is always spontaneously formed. However, even at very low temperature (160 K) the adsorption system evolves quickly to M-Oup. After the latter structure is formed, the system is stable even at the comparatively high temperature of 260 K, and due to the presence of the H-bond (~1.6 Å) between O_{2c}H and the O of

TABLE 2: Structural Parameters and Adsorption Energies of Dissociated Formic Acid on the Ridge of Reconstructed Anatase TiO_2(001)-1 × 4[a]

	$Ti_{4c}-O_f$ (Å)	$Ti_{4c}-O_{2c}$ (Å)	Ti_{4c}*$-O_{2c}$ (Å)	$O_{2c}-H_f$ (Å)	E_a (eV)	Figure
M-Hup	2.027	2.086	1.983	1.080	1.31	4a
M-Oup	1.911	3.703	1.776	1.013	1.66	4b
BC	2.209	2.300	1.943	0.994	2.15	4c

[a] Ti_{4c} is the 4-fold Ti at the ridge binding formate. Ti_{4c}* is the Ti at the ridge that binds O_{2c}, which accepts the acidic H (H_f) from formic acid. O_f is the O of formate that binds to Ti_{4c}; in the bidentate case, it represents both its O atoms and $Ti_{4c}-O_f$ is then the average bond distance.

formate binding to Ti_{4c}, rotation of formate or other transformation is hindered.

The most stable species on the 1 × 4 surface is the bidentate chelating BC species in Figure 4c. Here the geometry of the adsorbed formate is very similar to that on the 1 × 1 surface, for example, the average $O-Ti_{4c}$ bond distance is ~2.21 Å vs ~2.23 Å on the unreconstructed surface, but the calculated adsorption energy, 2.15 eV, is much higher than on the unreconstructed surface. Although BC is energetically more stable than M-Oup, a relatively high barrier seems to exist for the monodentate → bidentate transformation, which is actually not observed in our MD simulations even at a temperature of about 300 K. This is consistent with recent in situ FTIR work on anatase powders, which shows that the monodentate → bidentate transformation becomes significant only after the temperature is increased to more than 100 °C.[25] Therefore, under "mild" conditions, M-Oup is likely to be the majority species present on the surface.

The "standard" bidentate bridging configuration, BB1, is not allowed on the ridges of the reconstructed 1 × 4 surface. Instead, it is possible to have a bidentate configuration analogous to that in Figure 3e, in which the formate binds to two Ti_{4c} atoms linked via O_{2c}. However, the corresponding adsorption energy of 0.96 eV, similar to that on the 1 × 1 surface, indicates that this bidentate configuration is not favorable on the dry 1 × 4 surface either. In addition, formate in this structure sits in the middle between two Ti_{4c}, which does not agree with the experimental STM results (see below).[24]

Figure 4d shows the simulated STM image, calculated within the Tersoff−Hamann approach,[75] for M-Oup (at the maximum allowed coverage along the ridge). The surface formate appears as an oval constituted by two symmetric lobes and elongated perpendicular to the ridge, consistent with the shape of the lowest unoccupied molecular orbital (LUMO) of the adsorbed species.[24] The distance between two bright spots along the ridge, [100] direction, is 2*a*, that is, twice the lattice constant on the reconstructed surface. Moreover, since the surface formate sits closer to the Ti_{4c} to which it directly binds (Figure 4b), the bright oval is shifted from the center between the maxima along the ridge associated with the Ti_{4c} atoms. All these features replicate very well those found in recent room-temperature STM measurements.[24,26] On the other hand, as suggested by Tanner et al,[24] the calculated STM image for the BC configuration, shown in Figure 4e, is quite different from the experimental one: the bright oval spots are parallel, rather than perpendicular, to the ridge. This result further supports the argument we made above that M-Oup species dominate under mild conditions.

As expected, the terraces of the (001)-1 × 4 reconstructed surface are found to be much less reactive than the ridges. For example, HCOOH adsorption in monodentate configuration is found to be purely molecular on the terrace, with an adsorption energy of only ~0.9 eV, while dissociative adsorption in bidentate configuration gives an adsorption energy of less than 1 eV. Therefore, we may expect that formic acid adsorption on the 1 × 4 reconstructed surface occurs predominantly on the ridge, which is also supported by the STM work.[24]

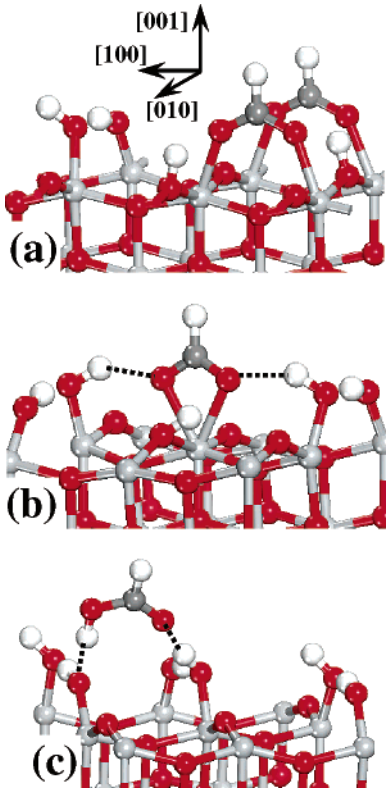

Figure 5. Possible structures of adsorbed formic acid in each p(3 × 2) surface cell of a (partially) hydrated anatase TiO_2(001)-1 × 1 surface: (a) $\theta_{H_2O} = 1/6$ ML, two BB1 species; (b) $\theta_{H_2O} = 1/3$ ML, BC; (c) $\theta_{H_2O} = 1/2$ ML (fully hydrated), physically adsorbed molecule. Dashed lines represent H-bonds.

5. Formic Acid Adsorption on Hydrated (001) Surfaces

5.1. Low Water Coverage. At water coverage $\theta_{H_2O} = 1/6$ ML, corresponding to one dissociated water molecule in each p(3 × 2) surface cell (Figure 1c), two HCOOH molecules may coadsorb dissociatively within the same surface cell. Among the many investigated systems, the energetically most favorable one, with two BB1 species (see Figure 5a), has an average adsorption energy per HCOOH of 1.46 eV, which is close to the adsorption energy for the same species on the clean surface. The corresponding structural parameters are given in Table 3.

5.2. High Water Coverage. At $\theta_{H_2O} = 1/3$ ML, M-Hup has a rather high adsorption energy of 1.26 eV, which is close to that on the clean surface (E_a = 1.19 eV). Due to obvious site competition, BB1 is precluded, while BC (Figure 5b), is very stable, with an adsorption energy, 1.54 eV, considerably higher than on the clean surface. This may be related to the presence of two H-bonds between the H of two surface OH groups sitting nearby and the two O of the adsorbed formate moiety. Thus it appears that surface hydration may selectively determine the nature of the adsorption complex.

TABLE 3: Structural Parameters and Average Adsorption Energies of Formic Acid on Partially Hydrated Anatase TiO_2(001)-1 × 1 at Water Coverages of $^1/_6$ and $^1/_3$ ML[a]

	θ_{H_2O}	$Ti_{5c}-O_f$ (Å)	$Ti_{5c}-O_{2c}$ (Å)	Ti_{5c}*$-O_{2c}$ (Å)	$O_{2c}-H_f$ (Å)	E_a (eV)	Figure
2 BB1	$^1/_6$ ML	2.093	2.040	2.035	0.991	1.46	5a
M-Hup	$^1/_3$ ML	2.073	2.364	1.821	1.138	1.26	
BC	$^1/_3$ ML	2.263	2.298	1.961	0.994	1.54	5b

[a] Atoms are labeled in the same way as in Table 1.

On the fully hydrated anatase TiO_2(001)-1 × 1 surface ($\theta_{H_2O} = {}^1/_2$ ML), there is no available chemisorption site for formic acid, so that only physical adsorption is feasible. From low-temperature (160 K) MD simulations, we obtained a relatively stable structure with HCOOH forming two H-bonds with surface OH groups (Figure 5c). The computed adsorption energy, 0.87 eV, is nearly identical to the adsorption energies of physically adsorbed CH_3OH and H_2O on fully hydrated anatase TiO_2(001)-1 × 1.[43] By combining this result with the difference in adsorption energy between chemisorbed H_2O/CH_3OH and HCOOH on the partially hydrated TiO_2(001)-1 × 1 surface,[43] we infer that formic acid should be able to irreversibly displace both water and methanol from the surface. In addition, the more straightforward dissociation process of HCOOH compared to that of the other two (reported in section 4.1) may also contribute to the easy replacement on the surface.

6. Conclusions

In this work, we have systematically studied formic acid adsorption on anatase TiO_2(001), the minority surface exposed by anatase TiO_2 nanoparticles, by taking into consideration the effects of coverage, surface hydration, and reconstruction. Our results can be summarized as follows.

(I) On both unreconstructed (1 × 1) and reconstructed (1 × 4) *clean* anatase TiO_2(001), formic acid dissociates spontaneously, yielding several species with rather large (∼1.5 eV) adsorption energies. Bidentate bridging species (BB) are the most favorable on the 1 × 1 surface, followed by bidentate chelating (BC) and monodentate ones. BC is particularly favored on the ridges of the 1 × 4 surface, where the computed adsorption energy is 2.15 eV. However, kinetics seems to favor the monodentate configuration, M-Oup, at intermediate temperatures. Indeed, the calculated STM image for this structure is in very good agreement with recent experimental STM results at room temperature.[24]

(II) On the partially hydrated 1 × 1 surfaces, formic acid still dissociates very easily and adsorbs in different configurations. Actually, the surface OH groups can drive adsorption from a BB to a BC mode, by hindering the former through site competition and stabilizing the latter through H-bonding. Furthermore, on the fully hydrated 1 × 1 surface, formic acid can physically adsorb in a relatively stable configuration.

(III) The above enumerated findings contrast with results of previous theoretical investigations on formic acid adsorption on the TiO_2 (anatase) (101) surface. This suggests that even though the (001) surface is a minority one, it could be very relevant in determining the chemistry of anatase nanoparticles.

(IV) On different anatase (001) surfaces and under a variety of conditions, formic acid in bidentate configurations always has much higher adsorption energies compared to water or methanol. Altogether, our results on the adsorption energetics of formic acid, water, and methanol are consistent with experimental observations on anatase colloidal nanoparticles,[22] namely that (i) water/methanol dissociative adsorption can occur reversibly and they can replace each other on the surface under the influence of their relative concentration in gas phase, and (ii) acetic acid, which is supposed to have adsorption characteristics very similar to those of formic acid, can irreversibly replace dissociated water and methanol.

Acknowledgment. This work is supported by the National Science Foundation (CHE-0121432). We gratefully acknowledge Pittsburgh Supercomputer Center and Keck Computational Materials Science Laboratory in Princeton for computing time. We thank U. Diebold for useful discussions.

Supporting Information Available: Structural parameters and charge-density distribution contours (PDF). This material is available free of charge via the Internet at http://pubs.acs.org.

References and Notes

(1) Diebold, U. *Surf. Sci. Rep.* **2003**, *48*, 53−229.
(2) Hagfeldt, A.; Grätzel, M. *Chem. Rev.* **1995**, *95*, 49−68.
(3) (a) Linsebigler, A. L.; Lu, G.; Yates, J. T., Jr. *Chem. Rev.* **1995**, *95*, 735−758. (b) Onda, K.; Li, B.; Zhao, J.; Jordan, K. D.; Yang, J. L.; Petek, H. *Science* **2005**, *308*, 1154−1158.
(4) Hoffmann, M. R.; Martin, S. T.; Choi, W.; Bahnemann, D. W. *Chem. Rev.* **1995**, *95*, 69−96.
(5) Rajh, T.; Saponjic, Z.; Liu, J. Q.; Dimitrijevic, N. M.; Scherer, N. F.; Vega-Arroyo, M.; Zapol, P.; Curtiss, L. A.; Thurnauer, M. C. *Nano Lett.* **2004**, *4*, 1017−1023.
(6) Fu, G. F.; Vary, P. S.; Lin, C.-T. *J. Phys. Chem. B* **2005**, *109*, 8889−8898.
(7) Wang, R.; Hashimoto, K.; Fujishima, A.; Chikuni, M.; Kojima, E.; Kitamura, A.; Shimohigoshi, M.; Watanabe, T. *Nature* **1997**, *338*, 431−432.
(8) Zhang, H. Z.; Banfield, J. F. *J. Mater. Chem.* **1998**, *8*, 2073−2076.
(9) Ranade, M. R.; Navrotsky, A.; Zhang, H. Z.; Banfield, J. F.; Elder, S. H.; Zaban, A.; Borse, P. H.; Kulkarni, S. K.; Doran, G. S.; Whitfield, H. J. *Proc. Natl. Acad. Sci. U.S.A.* **2002**, *99*, 6476−6481.
(10) Li, G.; Li, L.; Boerio-Goates, J.; Woodfield, B. F. *J. Am. Chem. Soc.* **2005**, *127*, 8659−8666.
(11) (a) Barnard, A. S.; Zapol, P.; Curtiss, L. A. *J. Chem. Theory Comput.* **2005**, *1*, 107−116. (b) Barnard, A. S.; Curtiss, L. A. *Nano Lett.* **2005**, *5*, 1261−1266.
(12) Barnard, A. S.; Zapol, P.; Curtiss, L. A. *Surf. Sci.* **2005**, *582*, 173−188.
(13) Martra, G. *Appl. Catal. A* **2000**, *200*, 275−285.
(14) Arrouvel, C.; Digne, M.; Breysse, M.; Toulhoat, H.; Raybaud, P. *J. Catal.* **2004**, *222*, 152−166.
(15) Dutta, P. K.; Ginwalla, A.; Hogg, B.; Patton, B. R.; Chwieroth, B.; Liang, Z.; Gouma, P.; Mills, M.; Akbar, S. *J. Phys. Chem. B* **1999**, *103*, 4412−4422.
(16) Nosaka, A. Y.; Fujiwara, T.; Yagi, H.; Akutsu, H.; Nosaka, Y. *J. Phys. Chem. B* **2004**, *108*, 9121−9125.
(17) Morterra, C. *J. Chem. Soc., Faraday Trans. 1* **1998**, *84*, 1617−1637.
(18) Henderson, M. A. *Langmuir* **1996**, *12*, 5093−5098.
(19) Araña, J.; Doña-Rodríguez, J. M.; González-Díaz, O.; Tello Rendón, E.; Herrera Melián, J. A.; Colón, G.; Navío, J. A.; Pérez Peña, J. *J. Mol. Catal. A* **2004**, *215*, 153−160.
(20) Araña, J.; Carriga i Cabo, C.; Doña-Rodríguez, J. M.; González-Díaz, O.; Herrera Melián, J. A.; Pérez Peña, J. *Appl. Surf. Sci.* **2004**, *239*, 60−71.
(21) (a) Schnadt, J.; Schiessling, J.; O'Shea, J. N.; Gray, S. M.; Patthey, L.; Johansson, M. K.-J.; Shi, M.; Krempaský, J.; Ahlund, J.; Karlsson, P. G.; Persson, P.; Mårtensson, N.; Brühwiler, P. A. *Surf. Sci.* **2003**, *540*, 39−54. (b) Schnadt, J.; O'Shea, J. N.; Patthey, L.; Schiessling, J.; Krempaský, J.; Shi, M.; Mårtensson, N.; Brühwiler, P. A. *Surf. Sci.* **2003**, *544*, 74−86.
(22) (a) Wang, C.-Y.; Groenzin, H.; Shultz, M. J. *J. Phys. Chem. B* **2004**, *108*, 265−272. (b) Wang, C.-Y.; Groenzin, H.; Shultz, M. J. *J. Am. Chem. Soc.* **2004**, *126*, 8094−8095. (c) Wang, C.-Y.; Groenzin, H.; Shultz, M. J. *J. Am. Chem. Soc.* **2005**, *127*, 9736−9744.
(23) Fein, D. E.; Wachs, I. E. *J. Catal.* **2002**, *210*, 241−254.

(24) Tanner, R. E.; Sasahara, A.; Liang, Y.; Altman, E. I.; Onishi, H. *J. Phys. Chem. B* **2002**, *106*, 8211−8222.
(25) Popova, G. Y.; Andrushkevich, T. V.; Chesalov, Y. A.; Stoyanov, E. S. *Kinet. Catal.* **2000**, *41*, 805−811.
(26) Tanner, R. E.; Liang, Y.; Altman, E. I. *Surf. Sci.* **2002**, *506*, 251−271.
(27) Herman, G. S.; Dohnálek, Z.; Ruzycki, N.; Diebold, U. *J. Phys. Chem. B* **2003**, *107*, 2788−2795.
(28) Hägglund, C.; Kasemo, B.; Österlund, L. *J. Phys. Chem. B* **2005**, *109*, 10886−10895.
(29) Chuang, C.-C.; Chen, C.-C.; Lin, J.-L. *J. Phys. Chem. B* **1999**, *103*, 2439−2444.
(30) Beck, D. D.; White, J. M.; Ratcliffe, C. T. *J. Phys. Chem.* **1986**, *90*, 3123−3131.
(31) Maira, A. J.; Coronado, J. M.; Augugliaro, V.; Yeung, K. L.; Conesa, J. C.; Soria, J. *J. Catal.* **2001**, *202*, 413−420.
(32) Szczepankiewicz, S. H.; Colussi, A. J.; Hoffmann, M. R. *J. Phys. Chem. B* **2000**, *104*, 9842−9850.
(33) Connor, P. A.; Dobson, K. D.; McQuillan, A. J. *Langmuir* **1999**, *15*, 2402−2408.
(34) Amore Bonapasta, A.; Filippone, F. *Surf. Sci.* **2005**, *577*, 59−68.
(35) (a) Tilocca, A.; Selloni, A. *J. Chem. Phys.* **2003**, *119*, 7445−7450. (b) Tilocca, A.; Selloni, A. *Langmuir* **2004**, *20*, 8379−8384. (c) Tilocca, A.; Selloni, A. *J. Phys. Chem. B* **2004**, *108*, 4743−4751. (d) Tilocca, A.; Selloni, A. *J. Phys. Chem. B* **2004**, *108*, 19314−19319.
(36) Selloni, A.; Vittadini, A.; Grätzel, M. *Surf. Sci.* **1998**, *402*−*404*, 219−222.
(37) Vittadini, A.; Selloni, A. *J. Phys. Chem. B* **2004**, *108*, 7337−7343.
(38) (a) Bredow, T.; Jug, K. *J. Phys. Chem.* **1995**, *99*, 285−291. (b) Bredow, T.; Jug, K. *Surf. Sci.* **1995**, *327*, 398−408. (c) Homann, T.; Bredow, T.; Jug, K. *Surf. Sci.* **2004**, *555*, 135−144.
(39) Vittadini, A.; Selloni, A.; Rotzinger, F. P.; Grätzel, M. *J. Phys. Chem. B* **2000**, *104*, 1300−1306.
(40) Vittadini, A.; Selloni, A.; Rotzinger, F. P.; Grätzel, M. *Phys. Rev. Lett.* **1998**, *81*, 2954−2957.
(41) Nilsing, M.; Lunell, S.; Persson, P.; Ojamäe, L. *Surf. Sci.* **2005**, *582*, 49−60.
(42) Mguig, B.; Calatayud, M.; Minot, C. *J. Mol. Struct. (THEOCHEM)* **2004**, *709*, 73−78.
(43) Gong, X.-Q.; Selloni, A. *J. Phys. Chem. B* **2005**, *109*, 19560−19562.
(44) Patthey, L.; Rensmo¸ H.; Persson, P.; Westermark, K.; Vayssieres, L.; Stashans, A.; Petersson, A.; Brühwiler, P. A.; Siegbahn, H.; Lunell, S.; Mårtensson, N. *J. Chem. Phys.* **1999**, *110*, 5913−5918.
(45) (a) O'Regan, B.; Grätzel, M. *Nature* **1991**, *353*, 737−740. (b) Nazeeruddin, Md. K.; Humphry-Baker, R.; Liska, P.; Grätzel, M. *J. Phys. Chem. B* **2003**, *107*, 8981−8987.
(46) Ushiroda, S.; Ruzycki, N.; Lu, Y.; Spitler, M. T.; Parkinson, B. A. *J. Am. Chem. Soc.* **2005**, *127*, 5158−5168.
(47) Thomas, A. G.; Flavell, W. R.; Chatwin, C.; Rayner, S.; Tsoutsou, D.; Kumarasinghe, A. R.; Brete, D.; Johal, T. K.; Patel, S.; Purton, J. *Surf. Sci.* **2005**, *592*, 159−168.
(48) Ohno, T.; Sarukawa, K.; Matsumura, M. *New J. Chem.* **2002**, *26*, 1167−1170.
(49) Gao, Y.; Elder, S. A. *Mater. Lett.* **2000**, *44*, 228−232.
(50) Barnard, A. S.; Zapol, P. *Phys. Rev. B* **2004**, *70*, 235403.
(51) McCormick, J. R.; Zhao, B.; Rykov, S. A.; Wang, H.; Chen, J. G. G. *J. Phys. Chem. B* **2004**, *108*, 17398−17402.
(52) Lazzeri, M.; Vittadini, A.; Selloni, A. *Phys. Rev. B* **2001**, *63*, 155409.
(53) Diebold, U.; Ruzycki, N.; Herman, G. S.; Selloni, A. *Catal. Today* **2003**, *85*, 93−100.
(54) Sasahara, A.; Uetsuka, H.; Onishi, H. *Appl. Phys. A* **2001**, *72*, S101−S103.
(55) Sayago, D. I.; Polcik, M.; Lindsay, R.; Toomes, R. L.; Hoeft, J. T.; Kittel, M.; Woodruff, D. P. *J. Phys. Chem. B* **2004**, *108*, 14316−14323.
(56) Hayden, B. E.; King, A.; Newton, M. A. *J. Phys. Chem. B* **1999**, *103*, 203−208.
(57) Fukui, K.-I.; Onishi, H.; Iwasawa, Y. *Chem. Phys. Lett.* **1997**, *280*, 296−301.
(58) Onishi, H.; Iwasawa, Y. *Chem. Phys. Lett.* **1994**, *226*, 111−114.
(59) Morikawa, Y.; Takahashi, I.; Aizawa, M.; Namai, Y.; Sasaki, T.; Iwasawa, Y. *J. Phys. Chem. B* **2004**, *108*, 14446−14451.
(60) Gutiérrez-Sosa, A.; Martínez-Escolano, P.; Raza, H.; Lindsay, R.; Wincott, P. L.; Thornton, G. *Surf. Sci.* **2001**, *471*, 163−169.
(61) Munuera, G.; Gonzalez, F.; Moreno, F.; Prieto, J. A. In *Catalysis: Proceedings of the 5th International Congress on Catalysis*; Hightower, J. W., Ed.; North-Holland: Amsterdam, 1973; Vol. 2, p 1159.
(62) Kim, K. S.; Barteau, M. A. *Langmuir* **1988**, *4*, 945.
(63) Car, R.; Parrinello, M. *Phys. Rev. Lett.* **1985**, *55*, 2471−2474.
(64) (a) Perdew, J. P.; Burke, L.; Ernzerhof, M. *Phys. Rev. Lett.* **1996**, *77*, 3865−3868. (b) Vanderbilt, D. *Phys. Rev. B* **1990**, *41*, 7892−7895.
(65) Lazzeri, M.; Selloni, A. *Phys. Rev. Lett.* **2001**, *87*, 266105.
(66) Nosè, S. *Mol. Phys.* **1984**, *52*, 255−268.
(67) PWSCF: Baroni, S.; Dal Corso, A.; de Gironcoli, S.; Giannozzi, P. http://www.pwscf.org.
(68) Marsh, K. N., Ed. *Recommended Reference Materials for the Realization of Physicochemical Properties*; Blackwell: Oxford, U.K., 1987.
(69) Reuter, K.; Scheffler, M. *Phys. Rev. Lett.* **2003**, *90*, 046103.
(70) (a) Gong, X.-Q.; Liu, Z.-P.; Raval, R.; Hu, P. *J. Am. Chem. Soc.* **2004**, *126*, 8−9. (b) Gong, X.-Q.; Raval, R.; Hu, P. *Phys. Rev. Lett.* **2004**, *93*, 106104.
(71) Herman, G. S.; Sievers, M. R.; Gao, Y. *Phys. Rev. Lett.* **2000**, *84*, 3354−3357.
(72) Liang, Y.; Gan, S.; Chambers, S. A.; Altman, E. I. *Phys. Rev. B* **2001**, *63*, 235402.
(73) (a) Silly, F.; Castell, M. R. *Appl. Phys. Lett.* **2004**, *85*, 3223−3225. (b) Ohsawa, T.; Yamamoto, Y.; Sumiya, M.; Matsumoto, Y.; Koinuma, H. *Langmuir* **2004**, *20*, 3018−3020.
(74) Łodziana, Z.; Topsøe, N.-Y.; Nørskov, J. K. *Nature Mater.* **2004**, *3*, 289−293.
(75) Tersoff, J.; Hamann, D. R. *Phys. Rev. B* **1985**, *31*, 805−813.